# RADIS: a real-time anomaly detection intelligent system for fault diagnosis of marine machinery

Christian Velasco-Gallego[*, a] and Iraklis Lazakis[a]

[a] Department of Naval Architecture, Ocean and Marine Engineering, University of Strathclyde, 100 Montrose Street, G4 0LZ, Glasgow, United Kingdom

**Corresponding author**

Email address: christian.velasco@strath.ac.uk (Christian Velasco-Gallego)

**Coauthor**

Email address: iraklis.lazakis@strath.ac.uk (Iraklis Lazakis)

**Abstract**

By enhancing data accessibility, the implementation of data-driven models has been made possible to empower strategies in relation to O&M activities. Such models have been extensively applied to perform anomaly detection tasks, with the express purpose of detecting data patterns that deviate significantly from normal operational behaviour. Due to its preeminent importance in the maritime industry to adequately identify the behaviour of marine systems, the Real-time Anomaly Detection Intelligent System (RADIS) framework, constituted by a Long Short-Term Memory-based Variational Autoencoder in tandem with multi-level Otsu's thresholding, is proposed. RADIS aims to address the current gaps identified within the maritime industry in relation to data-driven model applications for enabling smart maintenance. To assess the performance of such a framework, a case study on a total of 14 parameters obtained from sensors installed on a diesel generator of a tanker ship is introduced to highlight the implementation of RADIS. Results demonstrated the capability of RADIS to be part of a diagnostic analytics tool that will promote the implementation of smart maintenance within the maritime industry, as RADIS detected an average of 92.5% of anomalous instances in the presented case study.

**Keywords:** anomaly detection, smart maintenance, ship systems, marine machinery, deep learning, intelligent real-time systems

**Nomenclature**

| | |
|---|---|
| **AAKR** | Auto Associative Kernel Regression |
| **AE** | Auto-Encoder |
| **BIC** | Bayesian Information Criterion |
| **CBM** | Condition-Based Maintenance |
| **CI** | Confidence Interval |
| **CNN** | Convolutional Neural Network |
| **DBN** | Deep Belief Network |
| **DBSCAN** | Density-Based Spactial of Applications with Noise |
| **DT** | Digital Twins |
| **EB** | Expected Behaviour |
| **EM** | Expectation Maximization |
| **EWMA** | Exponential Weighted Moving Average |
| **FPGA** | Field Programmable Gate Array |
| **GMMs** | Gaussian Mixture Models |
| **IoS** | Internet of Ships |
| **LSTM** | Long Short-Term memory |
| **MA** | Maintenance Analytics |
| **NN** | Neural Network |
| **NRMSE** | Normalised Root Mean Square Error |
| **O&M** | Operations and Maintenance |
| **OCSVM** | One-Class Support Vector Machine |
| **OLS** | Ordinary Least Squares |
| **PLS** | Partial Least Squares |
| **PHM** | Prognostics and Health Management |
| **RADIS** | Real-time Anomaly Detection Intelligent System |
| **RNN** | Recurrent Neural Network |
| **SA** | Sensitivity Analysis |
| **SPRT** | Sequential Probability Ratio Test |
| **VAE** | Variational Autoencoder |
| **XAI** | eXplainable Artificial Intelligence |

## 1. Introduction

The application of innovative technologies in the maintenance context has demonstrated its capabilities to enhance operations and maintenance practices, reduce costs, extend equipment lifetime, improve safety, protect the environment, and ensure quality, thus guaranteeing the prosperity of Condition-Based Maintenance (CBM) within this industrial sector. Such a strategy facilitates data accessibility to enable innovative data-driven strategies, while enhancing current practices in relation to Operations and Maintenance (O&M) activities within this industrial sector through the identification of change which could indicate developing faults (Raptodimos and Lazakis, 2018).

Accordingly, analysis can empower such strategies by implementing of Maintenance Analytics (MA) frameworks. As outlined by Karim et al. (2016), and Jasiulewicz-Kaczmarek and Gola (2019), MA is comprised of four interconnected time-line phases (maintenance descriptive analytics, maintenance diagnostic analytics, maintenance predictive analytics, and maintenance prescriptive analytics), the aim of which is the promotion of maintenance actions by improving the understanding of data and information.

As part of the maintenance diagnostic analytics, anomaly detection, which aims to detect data patterns that deviate significantly from normal operation behaviour, is implemented to perform fault detection. Its implementation has been identified as being of paramount importance due to its extensive application domains (Erhan et al., 2021), in such areas as in manufacturing (Ducharlet et al., 2020; Alaoui-Belghiti et al., 2019; Morariu et al. 2020), railway (Oliveira et al., 2019; Xue et al., 2019; Shi et al., 2019), and aerospace (Roy et al., 2018; Li et al., 2019; Imbassahy et al., 2020).

However, when the maritime sector is considered, only 2% of the classed ships operate under a Condition-Based Monitoring (CBM) scheme (Jaramillo Jimenez et al., 2020). This indicates the lack of maturity of this industrial sector within the maintenance analytics context, thus making the implementation of fault diagnosis for marine machinery inconsistent while preventive maintenance is still preferred (Lazakis et al., 2018). If the application of data-driven methodologies for the application of anomaly detection of marine machinery is considered, only 7 identified studies related to such a matter have been identified, 4 of them referring to the application of machine learning models, such as one-class support vector machine (Lazakis et al., 2019) or polynomial ridge regression model (Cheliotis et al., 2020) If deep learning methodologies are considered, only variational autoencoders have been analysed to perform the anomaly detection task (Ellefsen et al., 2020), which are unable to consider sequential patterns. Accordingly, a combination of VAE and LSTM is considered in this inquiry to analyse if the reconstruction process is enhanced by considered such temporal dependencies. Moreover, there is a lack of available data for marine machinery in academia due to the sensitive and confidential information that can be extracted. Thus, most of the research performed is either based on simulated data, such as the case study implemented by Ellefsen et al. (2020), or does not consider deep learning methodologies due to the amount of data required and their lack of transparency (Cheliotis et al., 2020). It can be considered, therefore, that there is a lack of analysis of fault diagnosis of marine machinery in real scenarios, thus averting some data preparation steps, such as data imputation and steady states' identification, which are fundamental when analysing real operational data (Velasco-Gallego and Lazakis, 2021; Velasco-Gallego and Lazakis, 2020; Cheliotis et al., 2019). If the steady states' identification is further analysed, it can be observed that, although it is considered a critical task when utilising data collected from marine machinery due to the emergence of non-operating periods, such as manoeuvring and engine transients, the implementation of such a task is usually performed manually. However, there is a need of implementing this pre-processing step automatically if real-time deployment is considered. Of all publications identified that consider the steady states identification as a pre-processing phase, only 3 of them implemented data-driven models (Perera and Mo, 2016; Dalheim and Steen, 2020; Velasco-Gallego and Lazakis, 2021). To continue contributing towards the implementation of such a task, a novel steady states' identification method based on the implementation of the first-order Markov chain, which has demonstrated promising results in analogous tasks, such as data imputation, (Velasco-Gallego and Lazakis, 2021), is assessed in this study. In addition, the resulting anomalies and normal instances are represented in form of images to analyse how image thresholding techniques can contribute in the "visually" detection and ranking of anomalies. Accordingly, image generation is applied by the estimation of the NRMSE matrix and multi-level Otsu's thresholding. Although time series imaging has been performed and presented promising results when applying forecasting (Li et al., 2020), there is no evidence that such a method has been performed within the anomaly detection task in the sector to the best of the authors' knowledge.

Hence, to overcome the limitations presented in the preceding paragraph, a real-time anomaly detection intelligent system for fault diagnosis of marine machinery (RADIS) is proposed. In this study, a Long Short-Term Memory (LSTM)-based Variational Autoencoder (VAE) Neural Network (NN) for anomaly detection performance is presented in tandem with image generation by the estimation of the NRMSE matrix and multi-level Otsu's thresholding. The focus of which is to address the anomaly detection task of marine systems. Although several studies have been performed related to the maritime industry, to the best of the authors' knowledge, there is no evidence that such an approach has been developed and implemented. Additionally, data pre-processing is comprehensively analysed due to its importance in guaranteeing the adequate performance of RADIS. Specifically, the analysis of a novel steady states' identification method is assessed.

The following paragraphs are structured as follows. Section 2 presents a literature review. Section 3 describes the proposed methodology. Section 4 reflects on the results obtained after implementing the proposed methodology through a case study. To finish, in Section 5, the conclusions are presented.

**2. Literature review**

The implementation of anomaly detection methodologies in sectors such as manufacturing, aerospace, and railways is wide and robust. Langone et al. (2015) demonstrated the applicability of implementing Least Squares Support Vector Machines (LS-SVMs). Yang et al. (2011) presented a hybrid feature selection scheme for unsupervised learning. Thirukovalluru et al. (2016) examined traditional handcrafted features and compared them with features learned by Deep Neural Networks (DNNs). Helbing and Ritter (2018) discussed recent applications of Artificial Neural Networks (ANNs) and Deep Learning (DL) approaches in the wind turbines sector. Shang et al. (2018) developed a recursive slow feature analysis. Di Maio et al. (2012) compared two unsupervised ensemble methods (fuzzy C-means and hierarchical trees). Predictions of multiple classifiers were combined to reduce variance of both results and bias. Amruthnath and Gupta (2018) tested the accuracy, performance, and robustness of a total of 5 unsupervised learning algorithms (PCA T2 statistic, Hierarchical clustering, K-Means, Fuzzy C-Means clustering, and model-based clustering). Harrou et al. (2019) introduced a fault diagnosis approach for monitoring photovoltaic systems. An anomaly detection approach was developed by implementing a model-based on the one-diode model to mimic the characteristics of the photovoltaic array and, subsequently, apply a one-class Support Vector Machine (1SVM) to residuals from the simulation model to detect faults. Zhang et al. (2016) analysed Deep Learning Network (DBN) to perform classification. Specifically, an ensemble of DBNs with Multi-Object Evolutionary Algorithm based on Decomposition (MOEA/D) is implemented to detect failure degradation. Yuan and Liu (2013) introduced manifold regularization based on semi-supervised learning to implement fault diagnosis.

Although anomaly detection techniques have been widely applied in analogous industrial sectors, only a total of nine articles were identified in the maritime domain, which suggests a lack of analysis and formalisation of anomaly detection approaches for the analysis of marine machinery behaviour. Aslam et al. (2020) provided a comprehensive survey of the Internet of Ships (IoS) paradigm as well as its key elements and its main characteristics. The paper presented an interesting review of automatic fault detection methodologies in the maritime industry and provided evidence of the importance of applying automatic and intelligent methods that detect and report faults. Lazakis et al. (2018) proposed a methodology for the monitoring and detection of operating anomalies in ship machinery based on a one-class Support Vector Machine (OCSVM). Brandsæter et al. (2017) presented a cluster-based anomaly detection methodology. This was based on an original methodology that was divided into two main steps: signal reconstruction, through the implementation of Auto Associative Kernel Regression (AAKR), and residual analysis, by performing Sequential Probability Ratio Test (SPRT). The methodology was then modified to include two new steps: cluster analysis, by the utilisation of the *k*-means algorithm, and the selection of a set of closest points per cluster, which would replace the original dataset as training set to reduce the computational cost. The proposed methodology is expanded in Brandsæter et al. (2019). Cheng X. et al. (2019) implemented a denoising filter based on Field Programmable Gate Array (FPGA) to apply fault feature extraction in gearbox vibration signals that contain strong noise. Precisely, a 50-stage low-pass filter design was implemented and proved to denoise gear fault vibration signal to diagnose the gearbox fault. Brandsæter and Vanem (2021) focused on unsupervised methods based on clustering in order to detect changes in the data streams. In specific, *k*-means clustering, Mixture of Gaussian models, density-based clustering, self-organising maps, and support vector machines were analysed. Sensor signals related to the main bearing condition were introduced for validation purposes. Coraddu et al. (2019) applied a total of two anomaly detection methods: support vector machines and *k*-Nearest Neighbour. Data from the Research Vessel The Princess Royal were considered for the case study. Ellefsen et al. (2019) (a) reviewed four well-established deep learning techniques applied in Prognostics and Health Management (PHM) systems: Deep Belief Network (DBN), Auto-Encoder (AE), Long Short-Term Memory (LSTM), and Convolutional Neural Network (CNN). Ellefsen et al. (2020) proposed a fault-type independent spectral anomaly detection algorithm for marine diesel engine degradation in autonomous ferries. The VAE was utilised as DNN, and thus trained on pre-processed normal operation data, the engine loads of which were merged into one context by applying a multi-regime normalization technique. Then, the trained VAE was used to estimate the velocity and the acceleration of the anomaly score at each time step in three fault types with different natures of degradation. Both the velocity and the acceleration were estimated dynamically to detect faults automatically when the estimations exceeded the threshold limits. Analogously, an unsupervised reconstruction-based fault detection algorithm was also presented in Ellefsen et al. (2019) (b), as supervised classifiers are highly complex to be implemented within the maritime industry due to the lack of fault labels. Hence, VAE was selected as a reconstruction model, which was implemented in two data sets of real-operational data from a marine diesel engine. Cheliotis et al. (2020) combined Expected Behaviour (EB) models with the Exponential Weighted Moving Average (EWMA) for fault detection. Four different regression models were assessed: Ordinary Least Squares (OLS) single linear regression, multiple linear ridge regression, OLS single polynomial regression, and multiple polynomial ridge regression. The estimated residuals were analysed in an EWMA control chart that contained upper and lower control limits to detect faults. Data preparation was of paramount importance in this study due to the characteristics of the raw data and the models that were implemented. Density-Based Spatial Clustering of Applications with Noise (DBSCAN) algorithm was applied effectively to remove outliers and transient states of operation, and thus induce its applicability when dealing with these types of data.

As it can be perceived in the preceding paragraph, various challenges identified within the maritime industry need to be addressed in relation to fault diagnosis of marine machinery. For instance, to the best of the authors' knowledge, none of the proposed frameworks deal with temporal dependencies. Moreover, most of the case studies performed are either simulated or do not consider large amounts of data, thus averting some critical data preparation steps, such as data imputation, data denoising, and steady states' identification, which are of preeminent importance when dealing with real scenarios. In relation to the framework capability of being deployed in real-time, most of the studies do not evidence such an aspect. Given this challenge, the contributions of this paper in relation to the application of fault diagnosis of marine machinery are expressed hereunder.

- The introduction of a LSTM-based VAE as part of RADIS. Although analogous methods have been implemented for anomaly detection in other sectors, there is still a lack of analysis and formalisation of deep learning methodologies within the maritime industry. Moreover, as stated in the preceding paragraph, none of the analysed fault diagnosis frameworks for the analysis of marine machinery consider the temporal dependencies. Therefore, by combining such approaches, it is expected that the reconstruction phase is enhanced with regards to the implementation of vanilla VAEs when time series data is being considering for analysis.

- The utilisation of image thresholding techniques for the detection of anomalies. Image generation through the estimation of the NRMSE matrix and multi-level Otsu's thresholding is proposed to investigate its applicability for the detection of anomalous values in time series data. The encoding of time series into images has demonstrated its competitive performance in automatically extracting features when performing forecasting (Li et al., 2020) or fault classification tasks (Fahim et al, 2021), for instance. Thus, to continue exploring the novel area of time series imaging to allow machines "visually" recognise and classify time series (Wang and Oates, 2015), image thresholding is introduced to "visually" detect and rank anomalies.
- The analysis of a novel steady states' identification method based on image generation by estimating the transition matrix obtained from the implementation of the first-order Markov Chain and connected component analysis. Based on the analysis of analogous studies, there is no evidence that such a pre-processing step is being performed prior to the implementation of their respective anomaly detection frameworks. However, due to the appearance of different operating conditions in real scenarios, such a process needs to be automated. Furthermore, real datasets usually contain both transient and idle states that need to be adequately identified and discarded. Accordingly, this contribution aims to address the challenge of averting the training of the semi-supervised anomaly detection model with either abnormal data or non-operational data.



## Methodology

The proposed methodology is graphically represented in Fig. 1. The first step refers to data pre-processing, which is of critical importance due to the characteristics of the data set. Subsequently, time series denoising is applied by the implementation of LSTM-based VAE NN. Accordingly, the NRMSE between the input time series and the generated time series is determined. By estimating such a coefficient for each generated time series, the NRMSE matrix is obtained. Therefore, if image thresholding is applied by considering multi-level Otsu's thresholding method, the anomalousness of each instance of all the analysed sequences can be determined, thus labelling the behaviour identified at each time step. The training process of such an approach has been performed offline, whereas the remaining steps have been performed online.

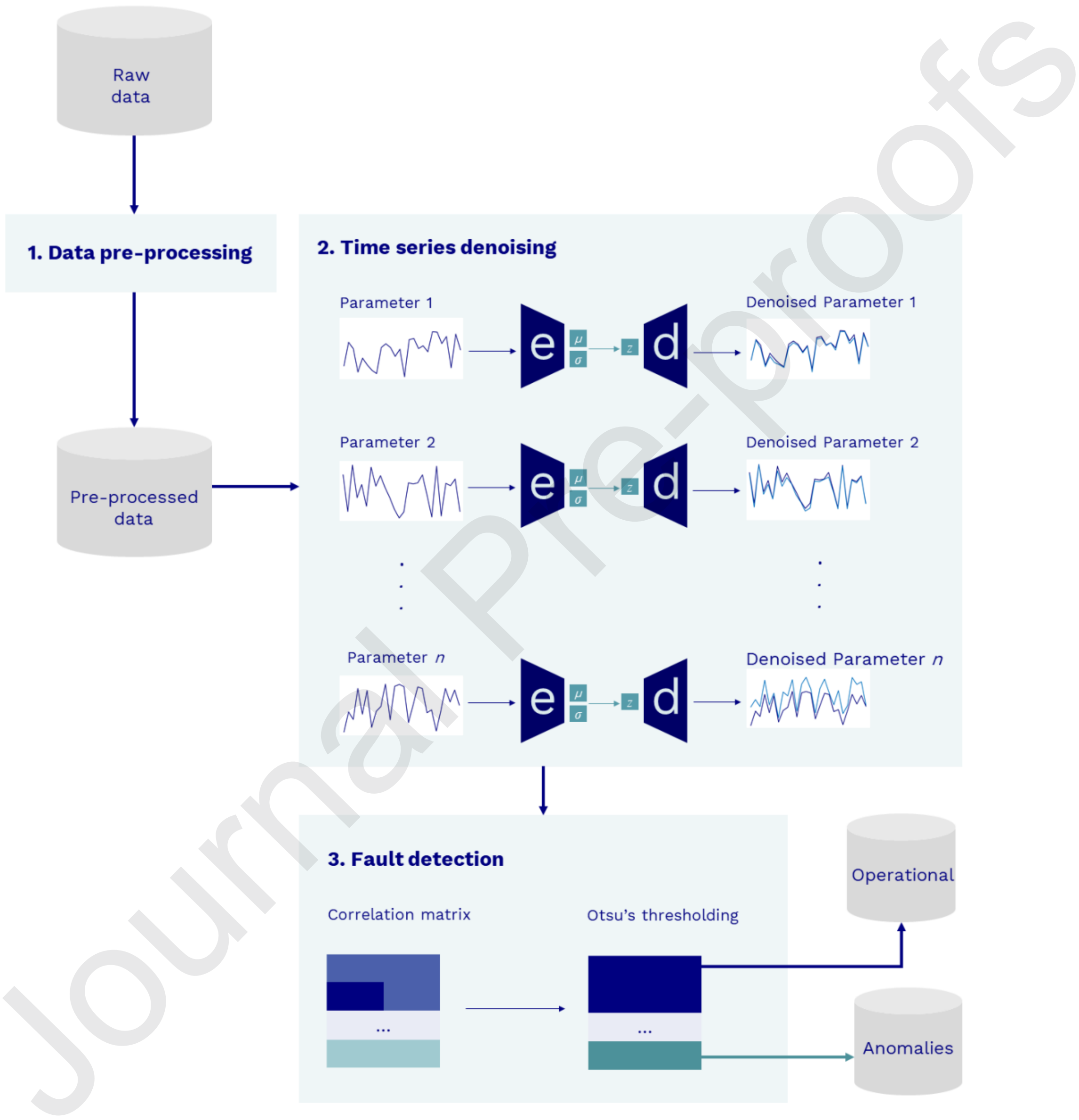


Fig. 1. Graphical representation of the proposed methodology.

### 3.1. Data pre-processing

To adequately apply pre-processing, a previous data understanding phase needs to be applied to establish the steps required based on the characteristics of the data set.

Raw data usually contain non-operational states that adversely alter the results outlined when performing data-driven tasks assessing the current and future health of marine machinery. Although the marine engines typically run under steady-state conditions, fluctuations may occur due to, for instance, environmental conditions or variations in the operating condition (Theotokatos et al., 2020). Therefore, if such states are not adequately addressed, a decrease in both computational efficiency and model effectiveness can be perceived. To that end, the methodology presented by Velasco-Gallego and Lazakis (2022) is analysed for identifying normal operational instances, and thus avert the training of the LSTM-based VAE with either abnormal instances or non-operational instances.

Such methodology is constituted by image generation of time series sensor data and connected component analysis. Firstly, the input time series is transformed into an image by the implementation of the first-order Markov chain. By applying such a process, it is determined that the occurrence at time *t* hinges only on the previous value and not on all values at time before $t$. Thus, if the time series values are clustered in a finite number of states, the first-order Markov chain transition matrix can be estimated, which will be considered as an image, and thus each of the pixels will be considered as an element of the matrix.

To estimate such a matrix, the definition of the discrete time stochastic process is considered. A discrete time stochastic process, $(X_n)_{n \in \mathbb{N}}$, which takes values in a finite set $S$, is considered to have the Markov property if the probability distribution of $X_{n+1}$ at time $n+1$ only hinges on the previous state $X_n$ at time $n$, and not on all the past values of $X_k$ for $k \leq n-1$. Thus,

$$\mathbb{P}(X_{n+1} = j \mid X_n = i_n,\ X_{n-1} = i_{n-1}, ..., Z_0 = i_0) = \mathbb{P}(Z_{n+1} = j \mid Z_n = i_n) = p(i,j) \quad (1)$$

where $i_0, i_1, ..., i_n, j \in S$.The probability $p(i,j)$ indicates the probability that the previous state $i$ is followed by the current state $j$. All the possible transition probabilities of a process can be collected in a $rxr$ matrix, where each $(i,j)$ entry $P_{ij}$ is $p(i,j)$,

$$\boldsymbol{P} = (P_{ij})_{1 \le i, j \le r} = \begin{pmatrix} p_{1,1} & p_{1,2} & \cdots & p_{1,r} \\ p_{2,1} & p_{2,2} & \cdots & p_{2,r} \\ \vdots & \vdots & \ddots & \vdots \\ p_{r,1} & p_{r,2} & \cdots & p_{r,r} \end{pmatrix} \quad (2)$$

and that satisfies

$$0 \le P_{ij} \le 1, \quad 1 \le i,j \le r, \quad (3)$$

$$\sum_{j=1}^{r} P_{ij} = 1, \quad 1 \le i \le r. \quad (4)$$

By considering the transition matrix estimated in the preceding step as a collection of discrete cells, a.k.a., pixels, the transformation from time series to image is achieved. Therefore, connected components labelling can be applied, in which the different connected components are clustered to identify the different states, and in turn determine those that only refers to steady states.

Additionally, input data normalisation is applied to yield values between -1 and 1. Each of the identified sequences is successively sectioned into subsequences by applying the sliding window algorithm. If required, data imputation can also be included within the data pre-processing step by implementing the methodologies proposed by Velasco-Gallego and Lazakis (2021), and Velasco-Gallego and Lazakis (2020).

### 3.2. Time series denoising

VAE, developed by Kingma and Welling (2013), is a generative algorithm capable of modelling the distribution of the data. This is a modification of an autoencoder that learns the parameters of a probability distribution. The model is constituted by a probabilistic encoder, which aims to learn both how to reduce the input dimensions and compress the inputs into an encoded representation. This compressed state, a.k.a. latent space representation, presents the lowest possible dimensions of the inputs. Subsequently, the decoder is utilised to learn how to reconstruct the data contained in the latent space representation to reproduce the inputs as analogously as possible. The architecture of such a model is described in Fig. 2.

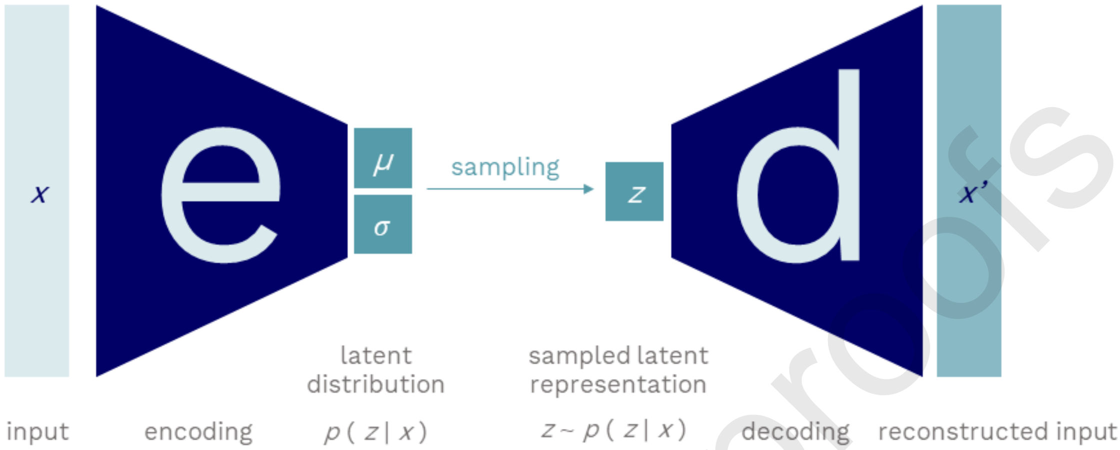


Fig. 2. VAE architecture.

The loss function being minimised is constituted by the reconstruction loss, which aims to ensure the efficient performance of the encoder-decoder arrangement, and the regularisation loss. The latter is determined by estimating the Kullback-Leiber divergence between the approximate posterior and prior latent variable *z*.

To consider the temporal dependences of sensor data of marine systems, the VAE approach is combined with LSTM in both the encoder and the decoder. LSTM is a type of Recurrent Neural Network (RNN) introduced by Hochreiter and Schmidhuber (1997) that learns long-term dependencies. As described in Fig. 3, the core component of such a network is the memory cell, which consists of a cell state vector and gating units, the latter regulating the information flow into and out of the memory, to maintain its state over time.

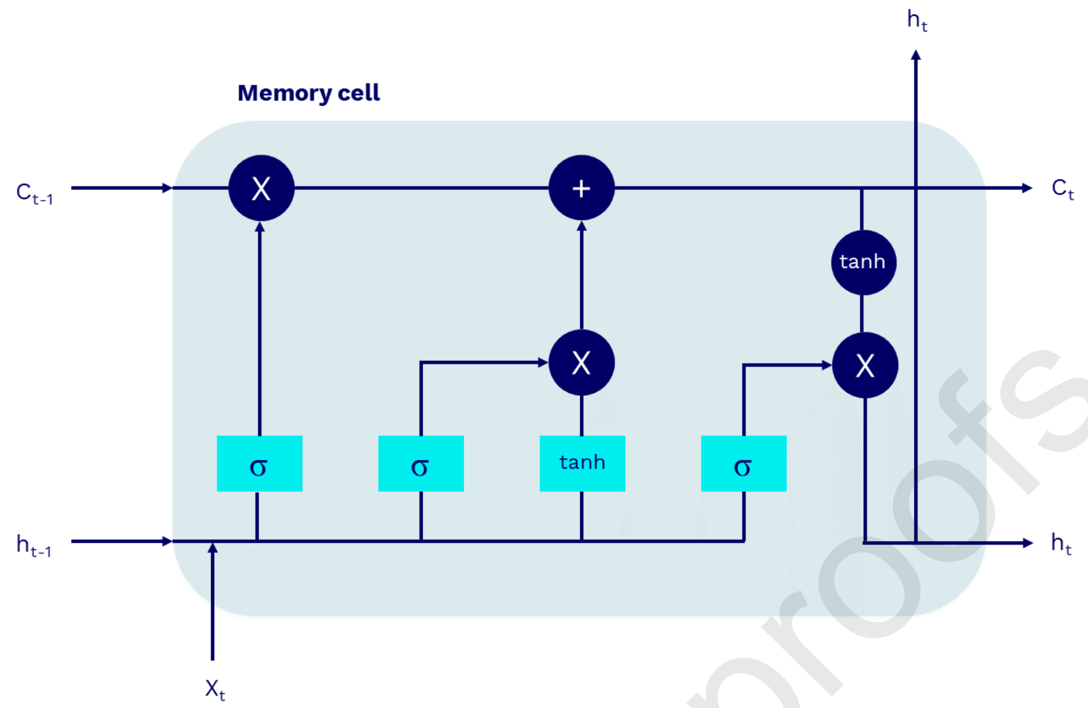


Fig. 3. LSTM cell architecture.

This step is performed by the implementation of the Python libraries Tensorflow and Keras.

### 3.3. Fault detection

By performing the preceding step, that is time series denoising, it is assumed that anomalous sequences will not be able to be properly reconstructed, and thus the resulting sequence will not be analogous to the observed one. Accordingly, the Normalised Root Mean Square Error (NRMSE) is estimated as presented in Eq. (5).

$$NRMSE = \frac{RMSE}{\bar{y}}, \tag{5}$$

where *RMSE* is the Root Mean Square Error (Eq. 6) and $\bar{y}$ is the mean of the observed values presented in the subsequence. The NRMSE has been utilised instead of the RMSE to facilitate the comparison of other parameters that present distinct scales.

$$RMSE = \sqrt{\frac{1}{n}\sum_{i=1}^{n}\left(y_i - \hat{y}_i\right)^2}, \tag{6}$$

where $n$ corresponds to the number of samples, and $y_i$ and $\hat{y}_i$ refer to the $i$-th occurrence of the observed and the predicted values of the subsequence.

Therefore, if such a value is estimated for every subsequence, a NRMSE matrix is achieved. Thus, as anomalous pixels will present distinct intensities over operational values, they can be adequately detected by applying image thresholding. This is a phase that segments the image into significantly distinct and non-overlapping homogenous regions (Anitha et al., 2021). For this inquiry, such a segmentation is performed by analysing the pixels' intensity and by considering a threshold-based technique. Specifically, the multi-level Otsu's method is applied. Such a method performs image thresholding by proposing a criterion for maximising the between-class variance of pixel intensity (Liao et al. (2001)). If the NRMSE matrix is considered as a 2D greyscale intensity function, it can be established that such an image contains a total of $N$ pixels with grey levels from 1 to $L$. The pixels' number with grey level $i$ is denoted as $f_i$. Thus, the probability of grey level $i$ in an image can be defined as expressed in Eq. (7).

$$p_i = \frac{f_i}{N} \tag{7}$$

By considering a total of $M$-$1$ thresholds, $\{t_1, t_2, ..., t_{M-1}\}$, which segments the initial image into $M$ classes: $C_1$ for $[1,...,t_1]$, $C_2$ for $[t_1+1,...,t_2]$, …, $C_i$ for $[t_{i-1}+1,...,t_i]$, …, and $C_M$ for $[t_{M-1}+1,...,L]$, the optimal thresholds $\{t_1{}^*, t_2{}^*, ..., t_{M-1}{}^*\}$ are selected by maximising the between-class variance, ${\sigma_B}^2$, as described hereunder.

$$\{t_1{}^*, t_2{}^*, ..., t_{M-1}{}^*\} = arg\max\{{\sigma_B}^2(t_1, t_2, ..., t_{M-1})\}, \quad 1 \le t_1 < ... < t_{M-1} < L \tag{8}$$

where

$${\sigma_B}^2 = \sum_{k=1}^{M} \omega_k (\mu_k - \mu_T)^2 \tag{9}$$

with

$$\omega_k = \sum_{i \in C_k} p_i, \tag{10}$$

$$\mu_k = \sum_{i \in C_k} \frac{ip_i}{\omega(k)}. \tag{11}$$

The $\omega_k$ in Eq. (9) relates to the zeroth-order cumulative moment of the $kth$ class $C_k$, and the numerator in Eq. (10) refers to the first-order cumulative moment of the $kth$ class $C_k$; that is,

$$\mu(k) = \sum_{i \in C_k} ip_i. \tag{12}$$

To adequately select the optimal number of classes, Gaussian Mixture Models (GMMs) with an Expectation Maximization (EM) algorithm is implemented.

**Results**

Having explored the methodology being analysed, a case study is introduced to assess its performance. Specifically, a Diesel GenSet of a tanker ship used for auxiliary needs is considered. This is a four-stroke in-line engine, comprised of a total of 6 cylinders. Further specifications are described in Table 1.

**Table 1.** Specifications of the analysed Diesel GenSet.

| | |
|---|---|
| Dimensions [L x W x H] (mm) | 6004 x 1600 x 2466 |
| Frequency (Hz) | 60 |
| Speed (rpm) | 900 |
| Power (kW) | 998 |
| Bore (mm) | 230 |
| Stroke (mm) | 300 |
| Cooling | Water-cooled |
| Cylinders | 6 |
| Weight (t) | 19.8 |
| Aspiration | Turbocharged |

The diesel generator power, the exhaust gas outlet temperature of each cylinder, the winding temperature (phases T, S, and R), the turbocharger exhaust gas outlet temperature, the cooling air temperature, the lubricating oil inlet temperature, and the cooling fresh water in pressure are analysed.

Such parameters are considered for this inquiry due to its critical importance in adequately monitoring the diesel generator being analysed to ensure its availability, whilst averting any operational issues. For instance, an anomaly detected in the winding temperature parameter may suggest the occurrence of overheating problems. That is to say, if the alternator overheats, the windings could burn out, thus altering their insulating properties. Another example is the monitoring of the exhaust gas temperature, as, if an increased is perceived, it could imply a malfunction of either the cooling system or the fuel system. Furthermore, other anomalous behaviours may occur in relation to the sensor being utilised, such as problems with the communications, sensor failure, or human error.

In total, more than 66,000 instances are analysed for each parameter, instances that have been collected in a 1-minute frequency. Fig. 4 represents graphically the time series raw data of the fourteen parameters being analysed. The descriptive statistics are also presented in Table 2.

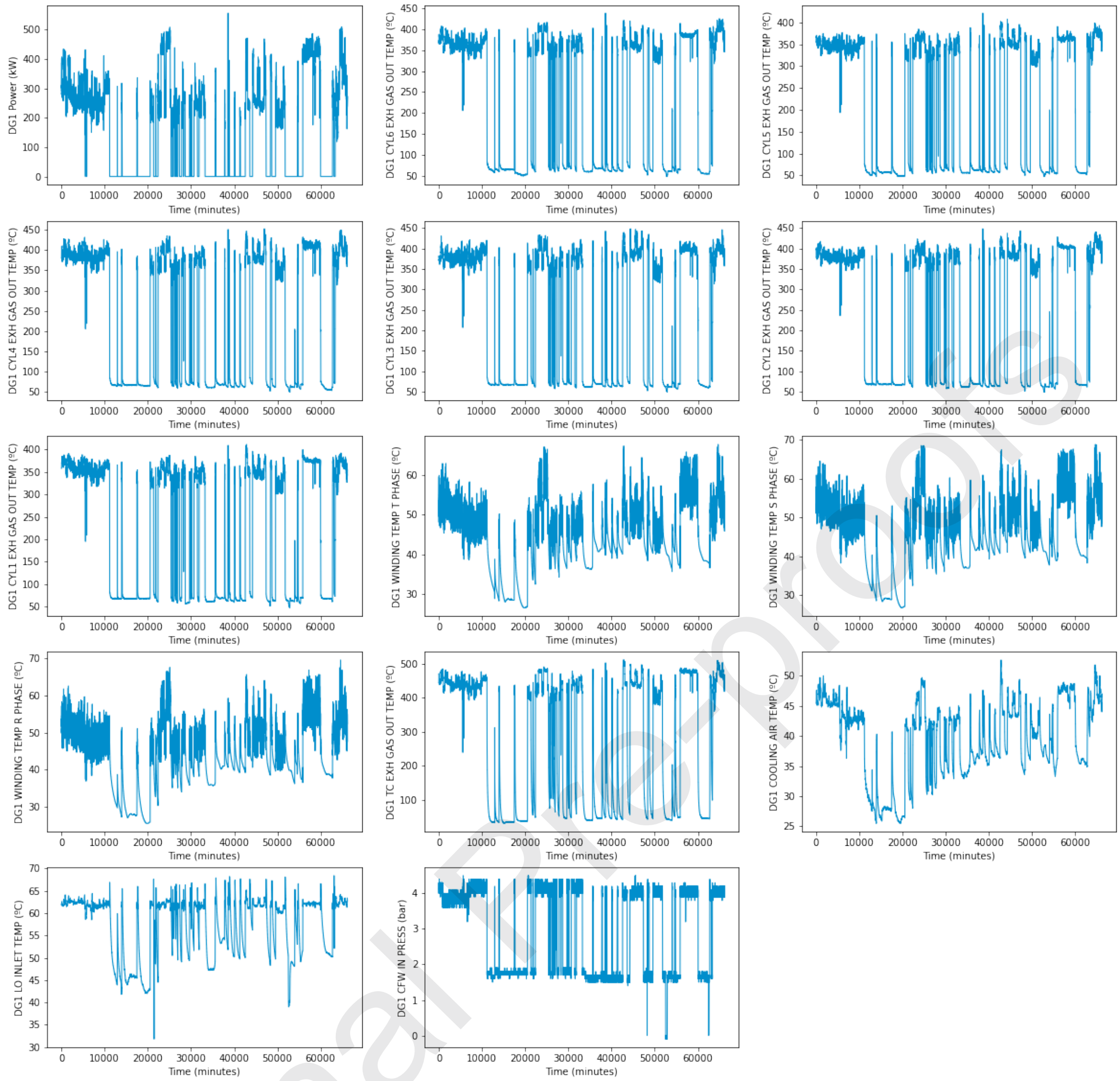


Fig. 4. Time series plot of the fourteen monitored parameters.

As it can be perceived, the distinct instances of the time series can be categorised in various states, such as idle states, transient states, and operational states of machinery. If Fig. 4 is further analysed, different adjustments can also be observed between operational states, which occur due to either contractual agreements between the charterer and the shipowner, relating to daily vessel speed and fuel oil consumption, or environmental conditions. Accordingly, steady states identification needs to be performed as part of the pre-processing step in order to consider those instances that refer to operational steady states only. For this inquiry, a total of 25 states have been considered when estimating the transition matrix. The categorisation of the time series instances of the diesel generator power parameter can be observed in Fig. 5.

**Table 2.** Descriptive statistics of the monitored parameters.

| Id | Parameter Name | Mean | Std. | Min. | 25% | 50% | 75% | Max. |
|---|---|---|---|---|---|---|---|---|
| 0 | Power (kW) | 151.67 | 159.15 | 0 | 0 | 177.9 | 273.2 | 555.9 |
| 1 | CYL6 EXH GAS OUT TEMP (ºC) | 222.68 | 153.00 | 48.1 | 64.3 | 329.7 | 370 | 438.7 |
| 2 | CYL5 EXH GAS OUT TEMP (ºC) | 209.99 | 144.67 | 47.6 | 58.4 | 309.8 | 351.3 | 421.1 |
| 3 | CYL4 EXH GAS OUT TEMP (ºC) | 231.52 | 160.16 | 48.5 | 65.7 | 336.8 | 386.5 | 453.1 |
| 4 | CYL3 EXH GAS OUT TEMP (ºC) | 230.16 | 157.23 | 48.7 | 67 | 330.7 | 383.8 | 448.1 |
| 5 | CYL2 EXH GAS OUT TEMP (ºC) | 231.68 | 158.10 | 48.5 | 67.3 | 344.9 | 383.3 | 448.5 |
| 6 | CYL1 EXH GAS OUT TEMP (ºC) | 215.61 | 143.68 | 47.1 | 67.5 | 312.1 | 355.4 | 411.7 |
| 7 | WINDING TEMP T PHASE (ºC) | 44.88 | 8.34 | 26.6 | 39.5 | 45.8 | 50.5 | 67.7 |
| 8 | WINDING TEMP S PHASE (ºC) | 46.11 | 8.80 | 26.7 | 40.6 | 47.3 | 51.9 | 68.8 |
| 9 | WINDING TEMP R PHASE (ºC) | 44.53 | 8.55 | 25.5 | 39.3 | 45.4 | 50.2 | 69.6 |
| 10 | TC EXH GAS OUT TEMP (ºC) | 263.94 | 190.23 | 31.6 | 49.4 | 384.7 | 444.2 | 510.1 |
| 11 | COOLING AIR TEMP (ºC) | 39.36 | 6.46 | 25.5 | 35.2 | 40.6 | 44.7 | 52.6 |
| 12 | LO INLET TEMP (ºC) | 57.30 | 6.62 | 31.8 | 51.4 | 61.3 | 62.1 | 68.4 |
| 13 | CFW IN PRESS (bar) | 2.91 | 1.20 | 0 | 1.7 | 3.8 | 4.1 | 4.5 |

If only operational sequences are assessed, a total of 81 are perceived. Each of these sequences have been further analysed to either accept or reject it for the training, validation, and test processes. If considered, the steady states identification methodology is applied again if the analysed sequence presents more than one steady state. Therefore, multiple iterations may need to be performed in order to obtain the optimal number of operational steady sequences.

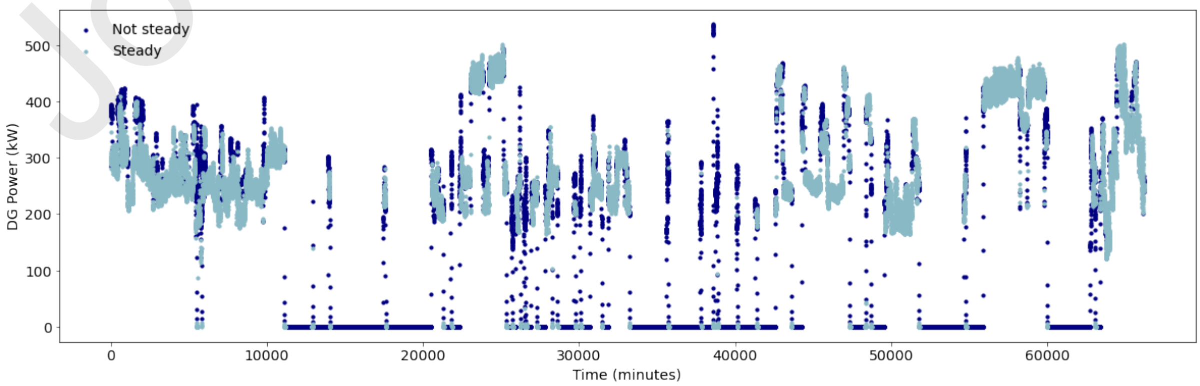


Fig. 5. Steady states identification for the diesel generator power parameter.

As part of the pre-processing phase, data normalisation is applied to each sequence to yield values between -1 and 1.

Once the pre-processing step is finalised, the LSTM-based VAE is applied to perform the time series reconstruction task. To that end, the grid search algorithm in tandem with *k*-fold cross-validation has been implemented to perform hyperparameter optimisation. Accordingly, a total of four hyperparameters have been considered (the number of layers in both encoder and decoder and their respective units, the number of latent dimensions, and the length of the sequences). The ranges analysed for each of the hyperparameters are specified in Table 3. The NRMSE metric has been considered to compare the results of each analysed combination. The selection of the sequence length is critical for the adequate performance of the model, as the greater is the length of the sequence the more the error is increased. This may indicate that the model may not adequately capture long dependences throughout the time series. Moreover, it has been perceived that when the number of units per layer and the number of latent dimensions is optimal, the benefit of considering multiple layers in both in the encoder and in the decoder is minimal. The same is perceived when many units per layer and latent dimensions is considered, as it has been perceived that by considering a total of 6 latent dimensions and 129 of units per layer the minimum RMSE value is achieved. Therefore, after analysing all the resulting architectures, the LSTM of both the encoder and decoder of the VAE-LSTM is formed by 1 layer (129 units) and tanh activation function. The number of latent dimensions is set to 6 and the sequence length to 3. Moreover, the ratio of the validation set has been set to 0.20. Adam optimizer has been applied to compile such a model. Subsequently, the model has been trained, setting the number of epochs to 100 and the batch size to 5. The main results obtained from the best set of hyperparameters is presented in Table 4.

**Table 3.** Range of values analysed for hyperparameter optimisation

| **Hyperparemeter** | **Range** |
|---|---|
| Number of layers in both encoder and decoder | (1, 2) |
| Number of units per layer | (2, 256) |
| Number of latent dimensions | (1, 24) |
| Length of sequences | (3, 180) |

**Table 4.** NRMSE results in the form of mean +- confidence interval (95%) of the best set of hyperparameters (validation set).

| | Folds | | | | |
|---|---|---|---|---|---|
| **Id** | **0** | **1** | **2** | **3** | **4** |
| 0 | 6.39e-04±5.49e-05 | 5.27e-04±3.36e-05 | 5.30e-04±2.48e-05 | 5.39e-04±4.68e-05 | 5.00e-04±2.86e-05 |
| 1 | 1.21e-04±1.89e-05 | 1.46e-04±1.66e-05 | 1.53e-04±1.65e-05 | 1.54e-04±2.69e-05 | 1.84e-04±1.80e-05 |
| 2 | 1.10e-04±1.44e-05 | 2.06e-04±1.56e-05 | 2.19e-04±1.75e-05 | 2.02e-04±3.22e-05 | 2.42e-04±2.03e-05 |
| 3 | 1.62e-04±1.84e-05 | 1.56e-04±1.88e-05 | 2.10e-04±2.31e-05 | 1.97e-04±2.66e-05 | 2.16e-04±1.99e-05 |
| 4 | 8.50e-05±1.32e-05 | 1.49e-04±1.73e-05 | 1.65e-04±1.50e-05 | 1.68e-04±2.05e-05 | 2.18e-04±2.23e-05 |
| 5 | 1.28e-04±1.69e-05 | 1.30e-04±1.57e-05 | 1.19e-04±1.47e-05 | 1.38e-04±2.34e-05 | 1.15e-04±1.24e-05 |
| 6 | 6.77e-05±9.49e-06 | 1.75e-04±1.82e-05 | 1.92e-04±2.12e-05 | 1.97e-04±3.96e-05 | 1.54e-04±1.72e-05 |
| 7 | 1.04e-03±6.37e-05 | 8.55e-04±4.61e-05 | 7.06e-04±3.65e-05 | 5.96e-04±4.53e-05 | 7.02e-04±3.42e-05 |
| 8 | 8.73e-04±5.73e-05 | 9.01e-04±4.54e-05 | 6.59e-04±3.61e-05 | 8.80e-04±7.34e-05 | 7.55e-04±3.87e-05 |
| 9 | 9.50e-04±5.99e-05 | 8.23e-04±4.33e-05 | 7.17e-04±4.01e-05 | 7.81e-04±5.65e-05 | 7.91e-04±4.99e-05 |
| 10 | 9.26e-05±1.41e-05 | 1.14e-04±1.31e-05 | 1.24e-04±9.70e-06 | 1.33e-04±1.89e-05 | 1.20e-04±1.55e-05 |
| 11 | 1.20e-04±1.00e-05 | 8.87e-05±1.17e-05 | 8.20e-05±1.41e-05 | 9.39e-05±4.32e-06 | 6.64e-05±7.19e-06 |
| 12 | 3.86e-05±3.55e-06 | 4.68e-05±1.26e-05 | 4.95e-05±1.41e-06 | 3.66e-05±2.76e-06 | 4.95e-05±7.27e-06 |
| 13 | 1.18e-03±4.16e-04 | 8.48e-04±6.56e-05 | 1.32e-03±8.16e-05 | 1.43e-03±2.40e-04 | 1.26e-03±8.60e-05 |

| | Folds | | | | |
|---|---|---|---|---|---|
| **Id** | **5** | **6** | **7** | **8** | **9** |
| 0 | 5.42e-04±3.00e-05 | 5.66e-04±3.82e-05 | 5.54e-04±3.68e-05 | 6.17e-04±8.98e-05 | 4.58e-04±2.40e-05 |
| 1 | 2.29e-04±2.36e-05 | 1.56e-04±2.50e-05 | 1.39e-04±2.07e-05 | 2.02e-04±4.66e-05 | 1.30e-04±1.50e-05 |
| 2 | 2.47e-04±2.71e-05 | 1.51e-04±2.09e-05 | 1.16e-04±2.28e-05 | 1.88e-04±5.14e-05 | 1.20e-04±2.27e-05 |
| 3 | 2.95e-04±2.67e-05 | 1.56e-04±2.71e-05 | 1.18e-04±1.61e-05 | 2.16e-04±5.00e-05 | 1.58e-04±1.89e-05 |
| 4 | 2.01e-04±2.14e-05 | 1.57e-04±2.13e-05 | 1.32e-04±1.65e-05 | 2.45e-04±6.21e-05 | 1.80e-04±2.04e-05 |
| 5 | 1.53e-04±1.67e-05 | 1.28e-04±1.93e-05 | 1.19e-04±1.65e-05 | 1.97e-04±6.73e-05 | 1.59e-04±2.39e-05 |
| 6 | 2.32e-04±2.61e-05 | 1.47e-04±2.64e-05 | 1.02e-04±1.87e-05 | 2.63e-04±7.39e-05 | 1.34e-04±1.81e-05 |
| 7 | 6.46e-04±3.34e-05 | 8.64e-04±5.74e-05 | 1.02e-03±6.53e-05 | 6.72e-04±6.63e-05 | 8.41e-04±5.45e-05 |
| 8 | 7.61e-04±3.96e-05 | 7.58e-04±4.89e-05 | 9.57e-04±7.06e-05 | 6.78e-04±6.41e-05 | 7.28e-04±5.02e-05 |
| 9 | 8.47e-04±4.28e-05 | 9.14e-04±5.99e-05 | 9.93e-04±6.61e-05 | 7.87e-04±7.86e-05 | 7.64e-04±4.67e-05 |
| 10 | 1.45e-04±1.72e-05 | 1.09e-04±1.65e-05 | 7.40e-05±1.03e-05 | 2.01e-04±7.58e-05 | 8.58e-05±1.08e-05 |
| 11 | 9.89e-05±1.14e-05 | 7.57e-05±4.58e-06 | 9.01e-05±1.30e-05 | 1.22e-04±6.75e-05 | 1.08e-04±8.43e-06 |
| 12 | 4.63e-05±6.98e-06 | 4.98e-05±4.01e-06 | 4.37e-05±6.06e-06 | 5.65e-05±1.12e-05 | 7.77e-05±4.19e-06 |
| 13 | 1.20e-03±7.26e-05 | 1.13e-03±1.14e-04 | 1.08e-03±8.22e-05 | 1.06e-03±2.03e-04 | 1.25e-03±9.26e-05 |

| Id | Average |
|---|---|
| 0 | 5.36e-04±1.14e-05 |
| 1 | 1.65e-04±6.87e-06 |
| 2 | 1.92e-04±7.59e-06 |
| 3 | 1.97e-04±7.79e-06 |
| 4 | 1.72e-04±6.95e-06 |
| 5 | 1.34e-04±6.16e-06 |
| 6 | 1.68e-04±7.83e-06 |
| 7 | 7.81e-04±1.52e-05 |

| | |
|---|---|
| 8 | 7.87e-04±1.57e-05 |
| 9 | 8.27e-04±1.66e-05 |
| 10 | 1.18e-04±5.59e-06 |
| 11 | 9.10e-05±4.42e-06 |
| 12 | 4.97e-05±2.35e-06 |
| 13 | 1.18e-03±4.40e-05 |

To assess the anomaly detection performance of the model, noise has been injected by considering different Gaussian distributions of various mean levels, analogous to how it had been performed in Zhao et al. (2019). Accordingly, the exhaust gas outlet temperature parameter of cylinder three has been altered to perform anomaly simulation, as, if an alteration of such a parameter is perceived it could imply a malfunction of either the cooling system or the fuel system. A total of 75 simulations have been performed, as it is considered that this number of simulations is appropriate to generally characterise the results. To simulate the real-time process, each instance of the time series has been provided in a 1-minute frequency basis, as this is the frequency at which data has been collected and provided by the ship operator. The average execution time of RADIS for detecting anomalies in an instance is 0.68 seconds (0.05 seconds per parameter). The hardware used consists of an Intel(R) Core (TM) i7-4790 CPU @ 3.60GHz 3.60 GHz and Windows 10. In total, 75 simulations have been performed in a sequence that has not been utilised for training purposes to ensure the generalisation capabilities of the proposed model. For the training process, a total of 65 sequences identified in the steady states' identification stage have been utilised, a total 20% of them being considered for validation purposes. The average NRMSE with a Confidence Interval (CI) of 95% obtained for each parameter is described in Fig. 7. Moreover, to complement such results and enhance visibility, the NRMSE obtained at each instance of the sequence for parameters 0 (power), 4 (exhaust gas outlet temperature of cylinder 3), which has been altered to simulate anomalies, and 9 (winding temperature at R phase), are also graphically represented in Fig. 8.

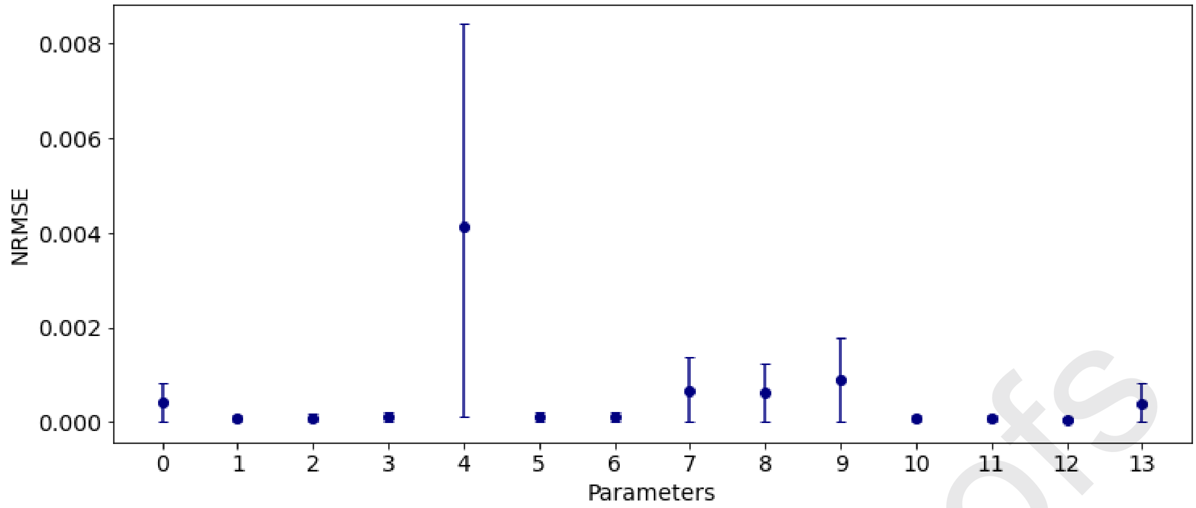


Fig. 7. Average NRMSE with CI 95% of the analysed parameters with injected anomalies in parameter 4.

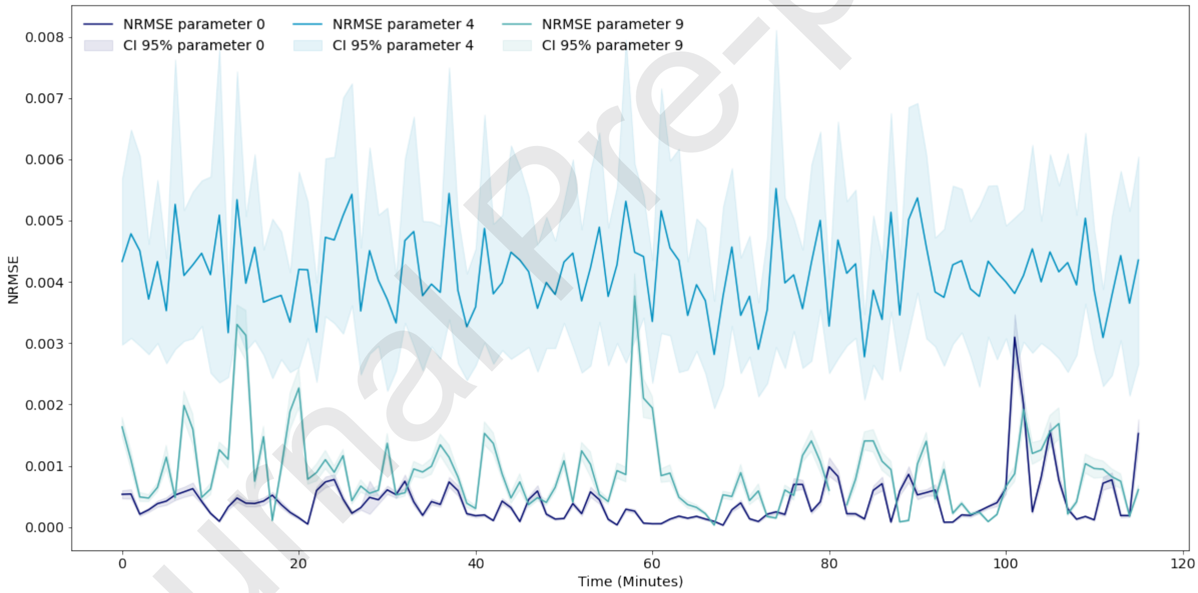


Fig. 8. NRMSE with CI 95% of parameters 0, 4, and 9 divided by instance with injected anomalies in parameter 4.

As observed in both figures, the injection of random noise to simulate anomalies in parameter 4 caused an increase in the reconstruction error, and thus an increment in the resulting NRMSE value. Such a fact is not observed in Figs. 9-10, in which parameter 4 has not been altered. In fact, parameter 4 presents analogous results in relation to the remaining parameters.

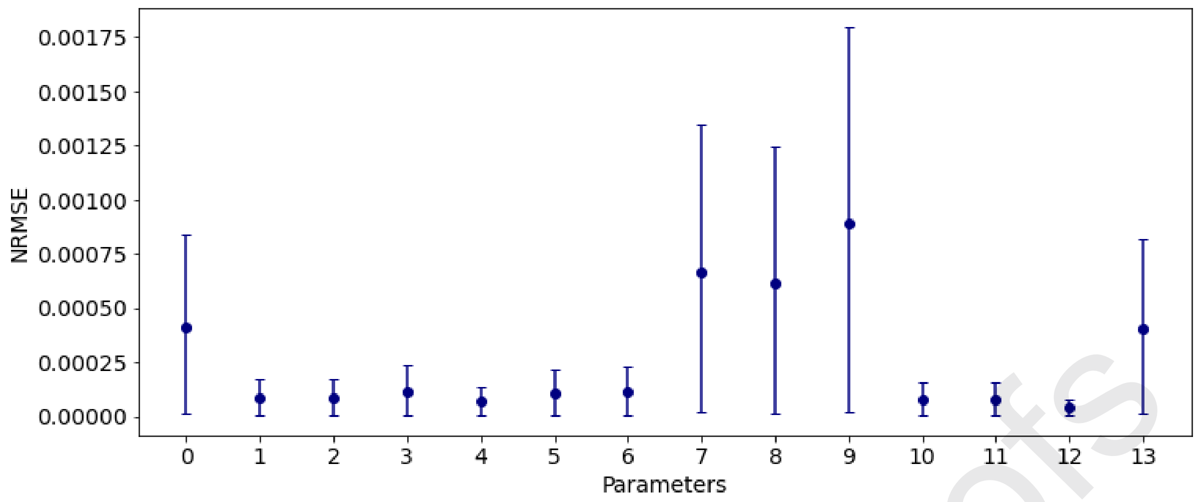


Fig 9. Average NRMSE with CI 95% of the analysed parameters.

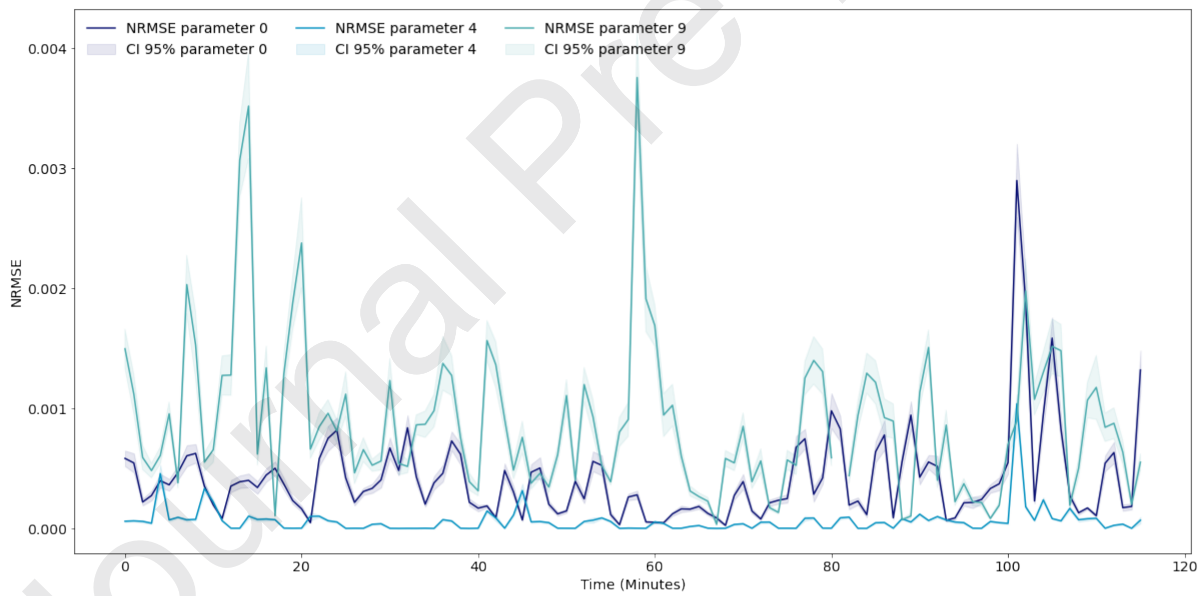


Fig 10. NRMSE with CI 95% of parameters 0, 4, and 9 divided by instance.

Accordingly, when performing image generation and scaling of the NRMSE values into the most common pixel format, the range of which varies between 0 and 255, it is expected that the pixels with higher intensity will refer to those parameters that present an anomalous value for that specific instance. By comparison, those parameters with non-anomalous values will constitute the pixels with the lowest intensity of the image (see Fig. 11). Therefore, image thresholding can be applied to not only automatically detect such anomalous values but also rank them depending on their level of anomalousness. Hence, possible relationships between parameters may be suggested for further analysis based on the resulting thresholding.

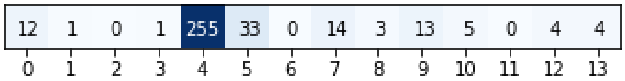


Fig 11. Image generated for instance 0 and simulation 0.

Specifically, multi-level Otsu's method is employed, as it is considered that image thresholding can adequately detect anomalies; anomalous pixels will present distinct intensities over operational values due to the results obtained in estimating the NRMSE between the reconstructed and observed subsequences. However, to implement such a method, the optimal number of classes needs to be specified. In this inquiry, GMMs with an EM algorithm is applied to assess its performance when selecting such classes. Therefore, Bayesian Information Criterion (BIC) is determined to identify the optimal number of components. Initial studies were conducted by considering a range of components between 1 and 10. However, it was perceived that multi-level Otsu's method was not efficient when a large number of classes were considered, making the implementation of this method in real time unfeasible. Accordingly, a bi-level thresholding task has been considered instead. Thus, $C_1$ refers to anomalous instances, while $C_2$ refers to normal instances. The selection of the number of classes for each sequence is applied by the implementation of the same approach, although the range of components between 1 and 2 is considered instead. Such a process has been performed to apply image thresholding in the generated images at each specific instance of the sequence and for each simulation performed. Once all the images were thresholded, the results were summarised by estimating the average accuracy, which is 92.5%. The proposed methodology presented promising results. However, as any other methodology, its limitations and disadvantages cannot be dismissed. The main limitations and disadvantages identified by the authors are presented hereunder.

- The steady states' identification is performed by the implementation of the first-order Markov chain. Thus, it is assumed that the time series follows the Markov property, and, therefore, the future states depend only on the current state. Moreover, the identification of steady states may be ineffective for short time intervals, as individual displacements are deterministically related in time (DelSole, 2000). Therefore, initial states in the analysed time series may not be identify appropriately.

- From the results obtained by the application of the grid search algorithm, the current version of the VAE-LSTM may not capture long dependencies throughout the time series. Therefore, further efforts need to be addressed in future research to overcome such a limitation.
- The Markov states and the hyperparameters of the VAE have been selected heuristically. More sophisticated methods need to be applied to optimise this step. Moreover, it has also been perceived that selection of the windows size when implementing the sliding window algorithm is critical for the success of RADIS.
- Multi-level Otsu's method may be unfeasible when it is implemented in real time if the number of classes are large. It has been perceived that the execution time when implementing multi-level thresholding is three time more than if bi-level thresholding is applied instead.
- The application of RADIS has been simulated so that such a methodology can be implemented in real time. However, the training of the proposed neural network is done offline. Moreover, as only a simulation has been performed to assess the real-time deployment of RADIS, a real-world case study needs to be performed to verify such an aspect. Thus, efforts in relation to inference acceleration, continuous training, and real-time deployment need to be met.

To guarantee the enhancement opportunities based on the results obtained from this inquiry, the following work guidelines are considered for further research:

- The analysis of optimisation techniques to adequately select the architecture of the deep neural network and sufficiently select the different hyperparameters of the applied models. The implemented grid search algorithm presented a significant computational cost for the analysis implemented, as only one potential area of a search space has been introduced. Therefore, further search spaces need to be considered to adequately perform the optimisation task. Moreover, as part of the future of research, evolutionary algorithms are expected to be also analysed to evaluate if the computational cost is reduced while the level of accuracy is either maintained or enhanced.

- The study of explainable artificial intelligence to provide further understanding in relation to the models' behaviour.
- The consideration of further anomaly contexts. For this inquiry, the addition of gaussian noise has been considered to alter the analysed sequences. However, it is of preeminent importance the analysis other contexts, such as degradations and contextual anomalies, which may be distinguished while performing diagnostic analytics.
- Time series similarity methods, including such measurements as transform-based similarity and time domain similarity, need to be analysed further prior to the implementation of image thresholding. Moreover, the extraction of statistical features may need to be considered as complementary to image thresholding as part of the fault diagnosis step.
- The implementation of ensemble methods for anomaly detection, as it is expected that by combining several anomaly detection techniques the performance of this task will be enhanced.
- The consideration of performance metrics to assess unsupervised learning. Although assumptions have been made to perform a semi-supervised learning task, the results obtained shows that the scenarios usually considered within the maritime industry are unsupervised. Accordingly, there is a need to study such metrics to ensure the efficient and effective performance of the proposed framework and enhance it.
- The exploration of weather and performance characteristics of the vessel to assess the possible enhancement of the proposed framework while providing support to ship owners, operators, and managers at a strategic level.



**Conclusions**

There is no doubt whatsoever about how data-driven models empower strategies in relation to O&M activities within the maritime sector. The application of anomaly detection techniques is merely one example. Such techniques, the aim of which is to detect data patterns that deviate significantly from normal operation behaviour, have been fundamental in sectors such as manufacturing, railway, and aerospace. However, when the maritime industry is considered, anomaly detection is, as yet a nascent practice. Consequently, further efforts need to be applied to implement innovative and collaborative tools that will facilitate the application of smart maintenance in this industrial sector.

Accordingly, RADIS is proposed, a Long Short-Term Memory-based Variational Autoencoder Neural Network for anomaly detection performance in tandem with image generation through estimation of the NRMSE matrix and multi-level Otsu's thresholding. To highlight and validate the performance of such a framework, a total of fourteen parameters collected from a diesel generator of a tanker ship was considered. Results demonstrated the capability of the proposed framework to detect anomalies that sensor data of marine machinery may contain. However, as expected, the performance of such an approach hinges on the characteristics of the anomalies, the utilisation of adequate pre-processing steps to ensure data quality, and the optimal definition of both the architecture and the training process of the model.

Thus, further research in this matter is of paramount importance, so that best practices can be established to ensure the adequate development of a real-time maintenance analytics tool to establish smart maintenance within the maritime industry. Examples of future guidelines that both industry and academia may need to consider are related to the analysis of optimisation techniques to adequately select the architecture of the deep neural network, the study of explainable artificial intelligence, the analysis of time series similarity methods, and the implementation of ensemble methods.

**Reference**

Alaoui-Belghiti A., Chevallier S., Monacelli E., 2019. Unsupervised Anomaly Detection Using Optimal Transport for Predictive Maintenance. Artificial Neural Networks and Machine Learning - ICANN 2019: Text and Time Series. ICANN 2019. Lecture Notes in Computer Science 11730, pp. 686-697, doi: https://doi.org/10.1007/978-3-030-30490-4_54.

Amruthnath N., Gupta T., 2018. A research study on unsupervised machine learning algorithms for early fault detection in predictive maintenance. 2018 5th International Conference on Industrial Engineering and Applications (ICIEA), pp. 355-361, doi: https://doi.org/10.1109/IEA.2018.8387124.

Anitha J., Pandian S. I. A., Agnes S. A., 2021. An efficient multilevel color image thresholding based on modified whale optimization algorithm. Expert Systems with Applications 178, pp. 1-19, doi: https://doi.org/10.1016/j.eswa.2021.115003.

Aslam S., Michaelides M. P., Herodotou H., 2020. Internet of Ships: A Survey on Architectures, Emerging Applications, and Challenges. IEEE Internet of Things Journal 7-10, pp. 9714-9727, doi: https://doi.org/10.1109/JIOT.2020.2993411.

Brandsæter A., Vanem E., Glad I. K. (2017). Cluster Based Anomaly Detection with Applications in the Maritime Industry. 2017 International Conference on Sensing, Diagnostics, Prognostics, and Control (SDPC), pp. 328-333, doi: https://doi.org/10.1109/SDPC.2017.69.

Brandsæter A., Vanem E., Glad I. K. (2019). Efficient on-line anomaly detection for ship systems in operation. Expert Systems With Applications 121, pp. 418-437, doi: https://doi.org/10.1016/j.eswa.2018.12.040.

Vanem, E., & Brandsæter, A. (2021). Unsupervised anomaly detection based on clustering methods and sensor data on a marine diesel engine. Journal of Marine Engineering & Technology, 20, doi: https://doi.org/10.1080/20464177.2019.1633223.

Calvo-Bascones P., Sanz-Bobi M. A., Welte T. M. I., 2021. Anomaly detection method based on the deep knowledge behind behavior patterns in industrial components. Application to a hydropower plant. Computers in Industry 125, pp. 1-17, doi: https://doi.org/10.1016/j.compind.2020.103376.

Cheliotis M., Gkerekos C., Lazakis I., Theotokatos G., 2019. A novel data condition and performance hybrid imputation method for energy efficient operations of marine systems. Ocean Engineering 188, pp. 1-14, doi: https://doi.org/10.1016/j.oceaneng.2019.106220.

Cheliotis M., Lazakis I., Theotokatos G., 2020. Machine learning and data-driven fault detection for ship systems operations. Ocean Engineering 216, pp. 1-17, doi: https://doi.org/10.1016/j.oceaneng.2020.107968.

Cheng X., Yang X., Chen Z. (2019). Research on FPGA filtering method of Gearbox fault signal. IOP Conference Series: Materials Science and Engineering 490, doi: https://doi.org/10.1088/1757-899x/490/5/052024.

Coraddu, A., Lim, S., Oneto, L., Pazouki, K., Norman, R., & Murphy, A. J. (2019). A novelty detection approach to diagnosing hull and propeller fouling. Ocean Engineering, 176, pp. 65-73, doi: https://doi.org/10.1016/j.oceaneng.2019.01.054.

Dalheim Ø. Ø., Steen S., (2020). A computationally efficient method for identification of steady state in time series data from ship monitoring. Journal of Ocean Engineering and Science 5, pp. 333-345, doi: https://doi.org/10.1016/j.joes.2020.01.003.

Dehestani D., Guo Y., Ling S. H., Su S. W., Nguyen H. T., 2012. Intelligent Fault Detection and Isolation of HVAC System Based on Online Support Vector Machine. Computational Intelligence and Its Applications, pp. 287-304, doi: https://doi.org/10.1142/9781848166929_0012.

Di Maio F., Hu J., Tse P., Pecht M., Tsui K., Zio E., 2012. Ensemble-approaches for clustering health status of oil sand pumps. Expert Systems with Applications 39, pp 4847-4859, doi: https://doi.org/10.1016/j.eswa.2011.10.008.

DelSole T., 2000. A Fundamental Limitation of Markov Models. Journal of the Atmospheric Sciences 57, pp. 1-11, doi: https://doi.org/10.1175/1520-0469(2000)057<2158:AFLOMM>2.0.CO;2.

Ducharlet K., Travé-Massuyès L., Le Lann M. V., Miloudi Y., 2020. A Multi-phase Iterative Approach for Anomaly Detection and Its Agnostic Evaluation. Trends in Artificial Intelligence Theory and Applications. Artificial Intelligence Practices. IEA/AIE, pp. 505-517, doi: https://doi.org/10.1007/978-3-030-55789-8\44.

Ellefsen A. L., Æsøy V., Ushakov S., Zhang, H. (2019) (a). A Comprehensive Survey of Prognostics and Health Management Based on Deep Learning for Autonomous Ships. IEEE Transactions on Reliability 68, pp. 720-740, doi: https://doi.org/10.1109/TR.2019.2907402.

Ellefsen A. L., Cheng X., Holmeset F. T., Æsøy V., Zhang, H, Ushakov S. (2019) (b). Automatic Fault Detection for Marine Diesel Engine Degradation in Autonomous Ferry Crossing Operation. IEEE International Conference on Mechatronics and Automation (ICMA) 2019, pp. 2195-2200, doi: https://doi.org/10.1109/ICMA.2019.8816600.

Ellefsen A. L., Han P., Cheng X., Holmeset F. T., Æsøy V., Zhang H., 2020. Online Fault Detection in Autonomous Ferries: Using Fault-Type Independent Spectral Anomaly Detection. IEEE

Transactions on instrumentation and measurement 69-10, pp. 8216-8225, doi: https://doi.org/10.1109/TIM.2020.2994012.

Erhan L., Ndubuaku M., Di Mauro M., Song W., Chen M., Fortino G., Bagdasar O., Liotta A., 2021. Smart anomaly detection in sensor systems: A multi-perspective view. Information Fusion 67, pp. 64-79, doi: https://doi.org/10.1016/j.inffus.2020.10.001.

Fahim S. R., Sarker S. K., Muyeen S. M., Sheikh M. R. I., Das S. K., Simoes M., 2021. A Robust Self-Attentive Capsule Network for Fault Diagnosis of Series-Compensated Transmission Line. IEEE Transactions on Power Delivery 36, pp. 3846-3857, doi: https://doi.org/10.1109/TPWRD.2021.3049861.

Harrou F., Dairi A., Taghezouit B., Sun Y., 2019. An unsupervised monitoring procedure for detecting anomalies in photovoltaic systems using a one-class Support Vector Machine. Solar Energy 179, pp. 48-58, doi: https://doi.org/10.1016/j.solener.2018.12.045.

Helbing G., Ritter M., 2018. Deep Learning for fault detection in wind turbines. Renewable and Sustainable Energy Reviews 98, pp. 189-198, doi: https://doi.org/10.1016/j.rser.2018.09.012.

Hochreiter S., Schmidhuber, J., 1997. Long short-term memory 9(8): pp. 1735-1780, doi: https://doi.org/10.1162/neco.1997.9.8.1735.

Imbassahy D. W. D., Marques H. C., Rocha G. C., Martinetti A., 2020. Empowering Predictive Maintenance: A Hybrid Method to Diagnose Abnormal Situations. Appl. Sci. 10, pp. 1-27, doi: https://doi.org/10.3390/app10196929.

Jasiulewicz-Kaczmarek M., Gola A., 2019. Maintenance 4.0 Technologies for Sustainable Manufacturing - an Overview. IFAC-PapersOnLine 52-10, pp. 91-96, doi: https://doi.org/10.1016/j.ifacol.2019.10.005.

Karim R., Westerberg J., Galar D., Kumar U., 2016. Maintenance Analytics - The New Know in Maintenance. IFAC-PapersOnLine 49-28, pp. 214-219, doi: https://doi.org/10.1016/j.ifacol.2016.11.037.

Kingma D. P., Welling M., 2013. Auto-encoding variational Bayes. arXiv.org, pp. 1-14, https://arxiv.org/abs/1312.6114.

Langone R., Alzate C., De Ketelaere B., Vlasselaer J., Meert W., Suykens J. A. K, 2015. LS-SVM based spectral clustering and regression for predicting maintenance of industrial machines. Engineering Applications of Artificial Intelligence 37, pp. 268-278, doi: https://doi.org/10.1016/j.engappai.2014.09.008.

Lazakis I., Gkerekos C., Theotokatos G. (2018). Investigating an SVM-driven, one-class approach to estimating ship systems condition. Ships and Offshore Structures 14:5, pp. 432-441, doi: https://doi.org/10.1080/17445302.2018.1500189.

Liao P-S., Chen T-S., Chung P-C., 2001. A fast algorithm for multilevel thresholding. Journal of Information Science and Engineering 17, pp. 713-727, url: http://citeseerx.ist.psu.edu/viewdoc/summary?doi=10.1.1.85.3669.

Li X., Zhang T., Liu Y., 2019. Detection of Voltage Anomalies in Spacecraft Storage Batteries Based on a Deep Belief Network. Sensors 19, pp. 1-21, doi: https://doi.org/10.3390/s19214702.

Li X., Kang Y., Li F., 2020. Forecasting with time series imaging. Expert Systems with Applications 160, pp. 1-13, doi: https://doi.org/10.1016/j.eswa.2020.113680.

Liu C., Gryllias K., 2020. A semi-supervised Support Vector Data Description-based fault detection method for rolling element bearings based on cyclic spectral analysis. Mechanical Systems and Signal Processing 140, pp. 1-24, doi: https://doi.org/10.1016/j.ymssp.2020.106682.

Lu H., Liu Y., Fei Z., Guan C., 2018. An Outlier Detection Algorithm Based on Cross-Correlation Analysis for Time Series Dataset. IEEE Access 6, pp. 53593-53610, doi: https://doi.org/10.1109/ACCESS.2018.2870151.

Jaramillo Jimenez V., Bouhmala N., Gausdal A. H., 2020. Developing a predictive maintenance model for vessel machinery. Journal of Ocean Engineering and Science 5, pp. 358-356, doi: https://doi.org/10.1016/j.joes.2020.03.003.

Madakyaru M., Harrou F., Sun Y., 2019. Monitoring Distillation Column Systems Using Improved Nonlinear Partial Least Squares-Based Strategies. IEEE Sensors Journal 19, pp. 11697-11705, doi: https://doi.org/10.1109/JSEN.2019.2936520.

Morariu C., Morariu O., Răileanu S., Borangiu T., 2020. Machine learning for predictive scheduling and resource allocation in large scale manufacturing systems. Computers in Industry, pp. 1-13 doi: https://doi.org/10.1016/j.compind.2020.103244.

Oliveira D. F. N., Vismari L. F., de Almeida J. R., Cugnasca P. S., Camargo J. B., Marreto E., Doimo D. R., de Almeida L. P. F, Gripp R., Neves M. M., 2019. Evaluating Unsupervised Anomaly Detection Models to Detect Faults in Heavy Haul Railway Operations. 2019 18th IEEE International Conference On Machine Learning and Applications (ICMLA), pp. 1016-1022, doi: https://doi.org/10.1109/ICMLA.2019.00172.

Perera L. P., Mo B., 2016. Data analysis on marine engine operating regions in relation to ship navigation. Ocean Engineering 128, pp. 163-172, doi: https://doi.org/10.1016/j.oceaneng.2016.10.029.

Raptodimos Y., Lazakis I., 2019. Using artificial neural network-self-organising map for data clustering of marine engine condition monitoring application. Ships and Offshore Structures 13, pp. 649-656, doi: https://doi.org/10.1080/17445302.2018.1443694.

Roy M. Bose S. K., Kar B., Gopalakrishnan P. K., Basu A., 2018. A Stacked Autoencoder Neural Network based Automated Feature Extraction Method for Anomaly detection in On-line Condition Monitoring. 2018 IEEE Symposium Series on Computational Intelligence (SSCI), doi: https://doi.org/10.1109/SSCI.2018.8628810.

Shang C., Yang F., Huang B., Huang D., 2018. Recursive Slow Feature Analysis for Adaptive Monitoring of Industrial Processes. IEEE Transactions on Industrial Electronics 65, pp. 8895-8905, doi: https://doi.org/10.1109/TIE.2018.2811358.

Shi W., Lu N., Jiang B., Zhi Y., Xu Z., 2019. An Unsupervised Anomaly Detection Method Based on Density Peak Clustering for Rail Vehicle Door System. 2019 Chinese Control and Decision Conference (CCDC), pp. 1954.1959, doi: https://doi.org/10.1109/CCDC.2019.8833427.

Theotokatos G., Stoumpos S., Bolbot V., Boulougouris E., 2020. Simulation-based investigation of a marine dual-fuel engine. Journal of Marine Engineering & Technology 19, pp. 1-13, doi: https://doi.org/10.1080/20464177.2020.1717266.

Thirukovalluru R., Dixit S., Sevakula R. K., Verma N. K., Salour A., 2016. Generating feature sets for fault diagnosis using denoising stacked auto-encoder. 2016 IEEE International Conference on Prognostics and Health Management (ICPHM), pp. 1-7, doi: https://doi.org/10.1109/ICPHM.2016.7542865.

Tian J., Azarian M. H., Pecht M., 2014. Rolling element bearing fault detection using density-based clustering. 2014 International Conference on Prognostics and Health Management, pp. 1-7, doi: https://doi.org/10.1109/ICPHM.2014.7036387.

Velasco-Gallego C., Lazakis I., 2020. Real-time data-driven missing data imputation for short-term sensor data of marine systems. A comparative study. Ocean Engineering 218, pp. 1-23., doi: https://doi.org/10.1016/j.oceaneng.2020.108261.

Velasco-Gallego C., Lazakis I., 2021. A novel framework for imputing large gaps of missing values from time series sensor data of marine machinery systems. Ships and Offshore Structures, pp. 1-11, doi: https://doi.org/10.1080/17445302.2021.1943850.

Velasco-Gallego C., Lazakis I., 2022. A real-time data-driven framework for the identification of steady states of marine machinery. Applied Ocean Research 121, pp. 1-12, doi: https://doi.org/10.1016/j.apor.2022.103052.

Xue L., Gao S., 2019. Unsupervised anomaly detection system for railway turnout based on GAN. Journal of Physics: Conference Series 1345, pp. 1-5, doi: https://doi.org/10.1088/1742-6596/1345/3/032069.

Yang Y., Liao Y., Meng G., Lee J., 2011. A hybrid feature selection scheme for unsupervised learning and its application in bearing fault diagnosis. Expert Systems with Applications 38, pp. 11311-11320, doi: https://doi.org/10.1016/j.eswa.2011.02.181.

Yuan J., Liu X., 2013. Semi-supervised learning and condition fusion for fault diagnosis. Mechanical Systems and Signal Processing 38, pp. 615-627, doi: https://doi.org/10.1016/j.ymssp.2013.03.008.

Zhang C., Sun J. H, Tan K. C., 2015. Deep Belief Networks Ensemble with Multi-objective Optimization for Failure Diagnosis. 2015 IEEE International Conference on Systems, Man, and Cybernetics, pp. 1-6, doi: https://doi.org/10.1109/SMC.2015.19.

Zhao Z., Cerf S., Birke R., Robu G., Bouchenak S., Mokhtar S. B., Chen L. Y., 2019. Robust Anomaly Detection on Unreliable Data. 49th Annual IEEE/IFIP International Conference on Dependable Systems and Networks (DSN), pp. 630-637, doi: https://doi.org/10.1109/DSN.2019.00068.